Calibration and Validation of the Angstrom-Prescott Model in Solar Radiation Estimation using Optimization Algorithms

Seyedeh Nafiseh Banihashemi Dehkordi[a], Bahram Bakhtiari[b], Kourosh Qaderi[b,*], Mohammad Mehdi Ahmadi[b]

[a] Ph.D. Candidate, Department of Water Engineering, Faculty of Agriculture, Shahid Bahonar University of Kerman, Kerman, Iran

[b] Associate Professor, Department of Water Engineering, Faculty of Agriculture, Shahid Bahonar University of Kerman, Kerman, Iran

ARTICLE INFO

Keywords:

Solar radiation

Sunshine

A-P model

Improved models

SCE algorithm

ABSTRACT

The Angstrom-Prescott (A-P) model is widely suggested for estimating solar radiation (R_s) in areas without measured or deficiency of data. The coefficients of this model must be locally calibrated, to calculate evapotranspiration (ET) correctly. The aim of this research was calibration and validation of the coefficients of the A-P model at six meteorological stations across arid and semi-arid regions of Iran. This model was improved by adding the air temperature and relative humidity terms. Besides, the coefficients ('a' and 'b') of the A-P model and improved models were calibrated using some optimization algorithms including Harmony Search (HS) and Shuffled Complex Evolution (SCE). Performance indices, i.e., Root Mean Square Error (RMSE), Mean Bias Error (MBE), and coefficient of determination (R^2) was used to analyze the models ability in estimating R_s. The results indicated that the performance of the A-P model had more precision and less error than improved models in all the stations. In addition, the best results were obtained for the A-P model with the SCE algorithm. The RMSE varies between 0.82 and 2.67 MJ m^{-2} day^{-1} for the A-P model with the SCE algorithm in the calibration phase. In the SCE algorithm, the values of RMSE had decreased about 4% and 7% for Mashhad and Kerman stations in the calibration phase compared to the HS algorithm, respectively. In other words, the highest decrease of RMSE is related to Kerman station.

* Corresponding author.
E-mail address: kouroshqaderi@uk.ac.ir

1. Introduction

The solar radiation (R_s) received from the Earth's surface is one of the most important factors affecting the thermal balance of the atmospheric-Earth system. The precise measurement or estimation of R_s is required for accurate design and management in irrigation and water resource planning and management, agriculture, meteorology, climatology, energy engineering, solar energy systems and especially in hydrology (Jahani et al. 2018; Liu et al. 2017; Robaa 2009). One of the major parts of the hydrological cycle is evapotranspiration (ET) process that is widely used for agricultural, irrigation management and water resources planning (Sanikhani et al. 2019). Solar radiation is the main input variable in the calculation of ET (Tabari et al. 2016; Boscaini et al. 2020). Due to the cost and the maintenance and calibration requirements of the R_s estimating instrument, and missing data or due to instrument failure or other related problems, it might be that the estimates of R_s are not available in several regions (Abraha et al. 2008; De Souza et al. 2016; Liu et al. 2001). For this reason, several methods have been presented to estimate R_s based on different types of methods such as satellite remote sensing (Sanchez-Lorenzo et al. 2017; Zhang et al. 2015), machine learning (Ağbulut et al. 2021; ,He et al. 2020; Kisi and Alizamir 2018; Shamshirband et al. 2015), numerical, and artificial intelligence (Jahani and Mohammadi 2018). There are some complexes and difficulties in using these methods for R_s estimation including requires many input variables; large datasets; coarse spatial resolution, and the eventuate model may not apply to other areas. Besides, there is no satellite-based database covering the study areas (Mihalakakou et al. 2000; , Şenkal and Kuleli 2009; Weiss and Hays 2004).

Another kind of method that has been developed and widely used for estimating R_s are empirical models (Fan et al. 2019). These models based on meteorological variables are a substitute to estimate R_s. Besides, these models using the easily accessible meteorological variables, such as sunshine duration, maximum and minimum air temperatures (T_{max}, T_{min}),

cloudiness, relative humidity ($RH_)$, and precipitation are attractive for its plainness, efficiency, and lower data requirement (Chen et al. 2018). Much preceding research has determinate that the sunshine-based models always outperform other types of models (Besharat et al. 2013; Chen et al. 2004). These models require relatively a few input variables and are easy to apply but it needs to calibrate their coefficients based on location and inputs data. However, the requirements to calibrate empirical models demonstrate that their coefficients are changing with locations. The station dependent coefficients limit the regional application of the empirical models, which is a big challenge for spatial rasterization. To solve this problem, the model coefficients for the regional usage must be calibrated.

Many models are developed for estimating R_s. One of the most famous empirical sunshine-based models is the Angstrom-Prescott (A-P) model. The A-P model has been applied to estimate global solar radiation based on measured sunshine hours. This model is widely used for its simpleness and remarkable performance (Paulescu et al. 2016; Raoof and Mobaser 2019; Sabziparvar and Shetaee 2007). One of the original constraints of the A-P model is that it requires calibration using local estimated R_s data. Where no measured values for global solar radiation are available in some stations, Angstrom prospered values of 0.2, and 0.5, and Prescott 0.22, and 0.54 for the empirical coefficients 'a' and 'b', respectively (Chen et al. 2013). Given its simpleness and premiere performance compared with other empirical models, its reference values for radiation coefficients 'a' and 'b', given by the Food and Agriculture Organization (FAO) Irrigation and Drainage Paper No. 56 (FAO56: a = 0.25, b = 0.5), can be used in cases where R_s data are not available (Allen et al. 1998; Chen et al. 2018; Liu et al 2019). Many research executed in various areas has shown that the use of the given coefficients to estimate R_s yields finite accuracy, and therefore, the coefficients of the A-P model should be calibrated locally (Liu et al. 2017; Sabziparvar et al. 2013; Tabari et al. 2016). FAO56 proposed the A-P model, which is a simple method to estimate the daily global solar radiation. The results of

previous researches showed that the application of the FAO pre-defined the A-P coefficients, for a variety of climatic and geographical conditions (without regardless of climate effect) the could challenge the validity of the FAO56-PM method (Liu et al. 2009; Yin et al. 2008). Therefore, many researchers performed a temporal and spatial calibration of 'a' and 'b' (Mousavi et al. 2014; Tabari et al. 2016). In another investigation, Aghashariatmadari et al. (2012) are calibrated the coefficients 'a' and 'b' and examined the variations of these coefficients at different time scales.

On the other hand, researchers have attempted to estimate R_s in addition to the sunshine, take advantage of other variables such as air temperature, relative humidity, cloudiness, saturation vapor pressure, and even precipitation (Chang and Zhang 2020; Jamil et al. 2019; Mousavi et al. 2014; Ododo et al. 1998).

Recently many kinds of meta-heuristic algorithms have been used to calibrate a different kind of empirical model in the real problem. Few usages of metaheuristic methods to solve solar energy problems have been reported; the Genetic Algorithm (GA) is one of these methods. Sen et al. (2001) have used GA for the designation of the A-P model coefficients. Harmony Search (HS) is one of the well-known and powerful optimization algorithms (Rahimi et al. 2012), which is emulating the music extemporization process where musicians extemporize their instruments' pitches searching for a perfect state of harmony, was developed by (Geem et al. 2001). The HS algorithm has been recently applied to different engineering optimization problems including optimized design of water dispensation network (Abualigah et al. 2020), optimal performance of a multi-reservoir system for hydropower and irrigation (Bashiri-Atrabi et al. 2015; Geem 2007), simulation of irrigation systems (Alshammari and Asumadu 2020;, Čistý 2007), an optimization model for groundwater management objectives (Luo et al. 2020), and recognition of unknown groundwater pollution sources (Ayvaz 2010). To fix the defects of the HS algorithm, the methods such as the Global Harmony Search (GHS) and Improved

Harmony Search (IHS) algorithm were developed. Another optimization algorithm that is used for effective global minimization and calibration of hydrologic models is the Shuffled Complex Evolution (SCE) algorithm (Duan et al. 1993). Also, this algorithm has been used widely for the calibration of different rainfall-runoff models (Adeyeri 2020), for the rehabilitation of water distribution networks (Elshaboury et al. 2020), and optimizing urban water supply Headwork's systems (Cui and Kuczera 2003).

There has not been much research on the computing R_s by optimization algorithms in Iran, and only one research conducted in Mashhad (Rahimi et al. 2012) examined. This is the first research by optimization algorithms for calibration of the A-P model coefficients in Iran. Through these algorithms, the A-P model coefficients are calibrated faster and more accurately, and R_s that is a fundamental input for calculating ET (Cunha et al. 2021), estimated more correctly. Accurate estimation of R_s provides an accurate calculate of ET. The exact calculation of ET is necessary for many applications such as improving water usage, agricultural planning, and effective water resources management, especially in arid and semi-arid climates.

This research aims to calibrate and improved the A-P model for estimating R_s at six meteorological stations in arid and semi-arid climates of Iran using the optimization algorithms including HS, IHS, GHS, and SCE. Then to investigate the effect of T and RH variables on the efficiency of the A-P model to estimating R_s, three improved A-P models were developed by adding terms of T_{max}, T_{min}, and mean relative humidity (RH_{mean}) and calibrated using applied optimization algorithms.

2. Material and methods

2.1.Study area

Iran is situated among latitudes of 25°N to 40°N and longitudes of 46°E to 65°E with an area of 1,648,000-km^2. Most parts of Iran are arid and semi-arid climates. On the other hand, low irrigation efficiency in agricultural fields requires that the amount of ET and water requirement

of plants that require an accurate estimate of the amount of R_s be calculated. In this research six meteorological stations, which are situated at arid and semi-arid climates of Iran, were selected to evaluate the performance of the calibrated A-P model in R_s estimation. The selected stations have arid and semi-arid climates based on the De Martonne climate classification method (Pellicone et al. 2019; Rahimi et al. 2013) from 1992–2017 and reliable long-term data (Fig. 1). The criteria for selection of the meteorological stations were based on the climate sort and the availability of the measured R_s.

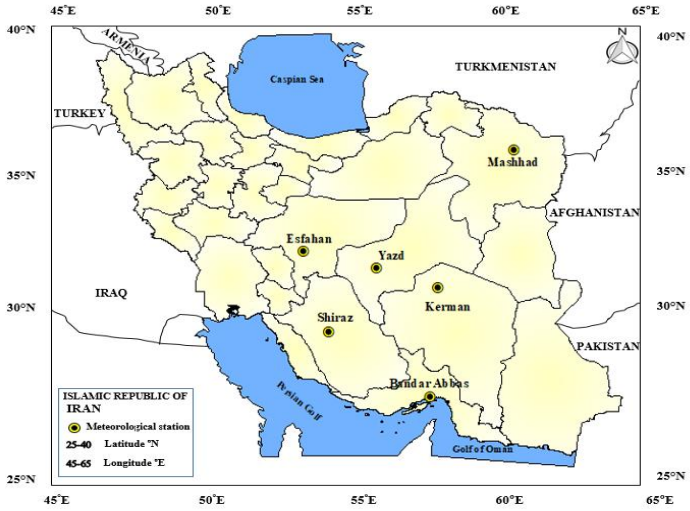

Fig. 1. Location of meteorological stations

2.2.Data and quality control

Daily meteorological data from six radiation stations were obtained from the Islamic Republic of Iran Meteorological Organization (IRIMO). The geographic and meteorological characteristics of the studied stations are presented in Table 1. In this research, the following meteorological characteristics were used as the inputs of the A-P and the three improved models: T_{max}, T_{min}, RH_{mean}, and R_s (MJ $m^{-2}day^{-1}$), maximum possible daily duration of sunshine hours (N), and mean the daily number of sunshine duration (n). Due to the importance of radiation data, the quality control of the observed daily global R_s was carried (Moradi 2009):

- If either the fluency index (R_s/R_a) or relative sunshine hours (n/N) were greater than one, the data for that day were deleted from the dataset.
- If R_s was greater than 0.78 × R_a, the data for that day were deleted from the dataset.
- If R_s was lower than 0.03× R_a, the data for that day were deleted.
- If there were ten or more days of lost data in the same month, the data for that month was omitted.

Table 1

Geographical and meteorological characteristics for the studied stations

station	Lat. (°N)	Lon. (°E)	Elev. (m)	Maximum Temperature (°c)	Minimum Temperature (°c)	Average sunshine (h)	Average R_s (MJ m^{-2} day^{-1})	RH (%)	Calibration period	climate	Validation period
Bandar Abbas	27.19	56.3	17	47	2.6	8.44	19.01	63.40	1992-2012	Semi-arid	2013-2017
Esfahan	32.46	51.66	1590	43	-19.3	8.6	16.74	35.92	1992-2012	Arid	2013-2017
Kerman	30.15	56.58	1754	41.4	-23.2	8.17	18.77	38.4	1992-2012	Arid	2013-2017
Mashhad	36.16	59.38	999	43.4	-21.37	7.27	16.24	53.98	1992-2012	Semi-arid	2013-2017
Shiraz	29.53	52.58	1486	42.4	-9	8.96	19.78	40.54	1992-2012	Semi-arid	2013-2017
Yazd	31.88	54.35	1222	45.6	-6.7	8.94	19.46	28.81	1992-2012	Arid	2013-2017

2.3.Models and optimization algorithms

2.3.1. Models

The A-P model is a model based on the sunshine, and to examine the effect of other meteorological variables, the following models presented in Table 2 were examined.

Table 2

Improved A-P model based on terms of T_{max}, T_{min}, and RH_{mean}

Models			Coefficients
Model1	Include air temperature	$R_s = [a_1 + b_1(n/N) + c\,(T_{max}-T_{min})]\,R_a$	a_1, b_1, c
Model2	Include relative humidity	$R_s = [a_2 + b_2\,(n/N) + d\,(RH_{mean})]\,R_a$	a_2, b_2, d
Model3	Combined Model 1 and Model 2	$R_s = [a_3 + b_3(n/N) + c_1\,(T_{max}-T_{min}) + d_1(RH_{mean})]\,R_a$	a_3, b_3, c_1, d_1

2.4.Optimization algorithm

The optimization algorithms were coded with MATLAB R2018a (9.4.0.813654). These algorithms are applied to find the optimal solution to a given calculational problem that

minimizes or maximizes a special function. In this research, optimization algorithms including SCE, IHS, GHS, and HS were used.

2.4.1. Shuffled Complex Evolution (SCE) algorithm

The SCE algorithm was expanded at the University of Arizona (Duan et al. 1992). Its strategy combines the strengths of the controlled random search (CRS) algorithms with the concept of competitive evolution (Holland 1975) and the newly modified concept of complex shuffling. The most important steps of the SCE are displayed in Fig. 2.

Initialize k, m and s = km
Sample $\{\theta_1, \ldots, \theta_s\}$, where $\theta_i \in \Theta$
Calculate function values $f_i = f(X, \theta_i)$ $i = 1, \ldots, s$
Sort f_i s.t. $k \leftarrow i$ and $f_1 \leq f_2 \leq f_k \leq f_{k+1} \ldots$
$D0 = \{(\theta_k, f_k), k = 1, \ldots, s\}$
Construct complexes C_j , $j = 1, \ldots, k$ s.t. $C_j = \{(\theta_k, f_k) \in D_0 | k = (j-1)_{m+1}, \ldots, j_m\}$
While Convergence Criteria do
  For j = 1: k do
    Evolve Cj using CCE (Competitive Complex Evolution)
  end for
  $D^l \leftarrow D^{l+1}$
  Go to 6
end while

Fig. 2. Pseudo-code of the SCE Algorithm

2.4.2. Harmony Search (HS) algorithm

When listening to a beautiful piece of classical music, who has ever wondered if there is any connector between music and finding an optimal solution to a tough design problem such as the water distribution networks or other design problems in engineering? Now for the first time, scientists have found such a fascinating connection by expanding a new algorithm, called HS. Geem et al. first expanded the HS in 2001.

- $$HM=\begin{bmatrix} x_{11} & x_{12} & x_{13} & \ldots & x_{1n} \\ x_{21} & x_{22} & x_{23} & \ldots & x_{2n} \\ \vdots & \vdots & \vdots & \vdots & \vdots \\ x_{HMS1} & x_{HMS2} & x_{HMS3} & \ldots & x_{HMSn} \end{bmatrix} \quad (1)$$

Harmony memory considering (HMC) rule:

- For this rule, a new random number r_1 is produced within the range [0, 1].

- If r_1 < HMCR, where HMCR is the harmony memory consideration rate, then the first decision variable in the new vector x_{ij}^{new} is elected randomly from the values in the present HM as follows:

- $x_{ij}^{new}=x_{ij},\ x_{ij}\epsilon\{x_{1j}, x_{2j}, x_{3j}, \ldots, x_{HMSj}\}$ (2)

The most important steps of the HS are displayed in Fig. 3

For each i ϵ [1, N] do
If U (0, 1) ≤ HMCR
$x'_i = x^i_j$, where j ~ U (1, 2, . . . , HMS).
If U (0, 1) ≤ PAR (pitch adjustment rate)
$x'_i = x_i \pm r \times bw$, where r ~ U (0, 1) and bw is an arbitrary distance bandwidth.
end if
else
$x'_i = LB_i + r \times (UB_i - LB_i)$, ($LB_i$ and UB_i are the lower and upper bounds for each decision variable, respectively)
end if

Fig. 3. Pseudo-code of the HS Algorithm

2.4.3. Developed Harmony Search (HS) algorithm

The HS is good at recognizing high-performance areas of the solution space in a sensible amount of time but gets difficult to do a local search for numeral usages. To improve the exact situation feature HS algorithm, IHS and GHS usage a new method that increases the precision setting and the convergence rate of HS. The IHS usages a new method to generate new solution vectors that increase the precision and convergence rate of the HS. Omran and Mahdavi (2008) suggested a new variation of HS, called GHS. First, in GHS, a dynamically updating scheme of parameter PAR usage in IHS (Mahdavi et al. 2007) is employed to improve the performance of GHS. Second, GHS modifies the pitch adjustment step of HS to use the best harmonic guidance information in harmony memory (HM). In the altered stage, GHS not only destroys the parameter bandwidth (BW), which is difficult to set because it can take any values in the range of [0,∞] but also introduces a social term of the best harmony with HS. These two methods (IHS, GHS) have been developed to overcome the disadvantages of the original method.

2.5.Methodology

One of the most popular empirical sunshine-based models is the A-P model. This model has been used to estimate global solar radiation based on measured sunshine hours. The model is as follows: (Angstrom 1924; Prescott 1940):

- $R_s = R_a [a + b(\frac{n}{N})]$ (3)

Where R_s and R_a is daily global solar radiation and daily extraterrestrial solar radiation (MJ m^{-2} day^{-1}), respectively, n is the mean daily number of sunshine duration (h), N is the maximum possible daily duration of sunshine hours (h) and 'a' and 'b' are empirical coefficients which must be calibrated based on long-term measured R_s data. R_a data for each day and location were gained from the estimation of geographical parameters including solar declination, solar constant, and the time of the year as shown in the method below (Allen et al. 1998):

- $R_a = 37.6 d_r [\omega_s \sin\emptyset \sin\delta + \cos\emptyset \cos\delta \sin\omega_s]$ (4)

Where d_r is the eccentricity correction factor of the Earth's orbit (equation (5)); ω_s is the sunshine hour angle of the sun at sunrise in radians (equation (6)), ϕ is the latitude of the station, and δ is the solar declination angle in radians equation(7):

- $d_r = 1 + 0.033 \cos (J_s \frac{360}{365})$ (5)
- $\omega_s = \arccos (-\tan\emptyset \tan\delta)$ (6)
- $\delta = 0.409 \sin (\frac{360}{365} J_s - 1.39)$ (7)

The maximum possible average daily length of sunshine hour N can be calculated by Duffie-Beckman 1991 model:

- $N = \frac{2}{15} \omega_s$ (8)

2.6.Performance indicators

The performance indicators discussed in this research were the coefficient of determination (R^2), Mean Bias Error {MBE (MJ $m^{-2}day^{-1}$)}, Root Mean Square Error {RMSE (MJ $m^{-2}day^{-1}$)}. These indicators were calculated as follows:

- $$R^2=\left[\frac{\sum_{i=1}^{m}(R_{estim}-\mu_{estim})(R_{meas}-\mu_{meas})}{\left[\sum_{i=1}^{m}(R_{estim}-\mu_{estim})^2\right]^{0.5}\left[\sum_{i=1}^{m}(R_{meas}-\mu_{meas})^2\right]^{0.5}}\right]^2 \quad (9)$$

- $$RMSE=\left[\frac{1}{M}\sum_{i=1}^{M}(R_{estim}-R_{meas})^2\right]^{1/2} \quad (10)$$

- $$MBE=\frac{1}{M}\sum_{i=1}^{M}(R_{estim}-R_{meas}) \quad (11)$$

Where M is the total number of estimated values, R_{estim} and R_{meas} are, respectively, estimated and measured daily global solar radiation values, μ_{estim} is the average of the daily estimated values and μ_{meas} is the average of the daily measured values. The R^2 stands for the proportion of variability in a data set that is calculated for by the model. The MBE, RMSE, and the R^2 statistical indices were used to evaluate the performance of applied optimization methods and improved the A-P model for R_s estimating. The negative values of MBE represent the difference between the estimated data and measured data. If the MBE value is positive, then the estimated values are overestimated and if the MBE value is negative, it means the underestimate of the estimated values. Whatever the MBE value is closer to zero indicates the accuracy of the model and the closeness of the amount of estimation data to the measured data.

3. Results and discussion

The calibrated coefficients for the A-P model and the models obtained with different optimization algorithms, the empirical coefficients (a, b, c, d) for four models, and the RMSE, R^2, MBE values are shown in Table 3 and Table 4 respectively.

Table 3

The locally calibrated of the models coefficients for the selected stations using optimization algorithms

station	Algorithm	A-P Model		Model1			Model2			Model3			
		a	b	a_1	b_1	c	a_2	b_2	d	a_3	b_3	c_1	d_1
Bandar Abbas	SCE	0.38	0.35	0.39	0.31	-0.0015	0.38	0.35	0	0.4	0.35	-0.0019	0
	HS	0.38	0.36	0.36	0.35	0.0036	0.47	0.33	-0.0012	0.3	0.38	0.0078	0.0002
	IHS	0.39	0.33	0.39	0.36	-0.0046	0.32	0.37	0.0008	0.29	0.33	0.0058	0.0012
	GHS	0.36	0.37	0.35	0.39	-0.0006	0.39	0.35	-0.0002	0.47	0.20	-0.0016	-0.0003
Esfahan	SCE	0.15	0.58	0.15	0.58	-0.0004	0.15	0.58	0	0.15	0.58	-0.0004	0
	HS	0.13	0.60	0.18	0.60	-0.0076	0.20	0.54	-0.0007	0.1	0.54	0.0152	-0.0008
	IHS	0.16	0.56	0.12	0.64	-0.0021	0.16	0.54	0.0005	0.15	0.57	-0.0006	0.0003
	GHS	0.15	0.57	0.14	0.59	0	0.13	0.59	0	0.12	0.63	0	0
Kerman	SCE	0.27	0.51	0.27	0.51	-0.0013	0.28	0.49	-0.0003	0.29	0.50	-0.0019	-0.0003
	HS	0.28	0.47	0.21	0.44	0.0109	0.18	0.59	0.0015	0.34	0.57	-0.0058	-0.0022
	IHS	0.24	0.54	0.32	0.46	-0.0025	0.38	0.41	-0.0012	0.19	0.58	-0.0011	0.0006
	GHS	0.26	0.50	0.28	0.50	-0.0013	0.30	0.48	-0.0006	0.36	0.50	-0.0061	-0.0009
Mashhad	SCE	0.22	0.62	0.22	0.62	-0.0001	0.23	0.61	0	0.23	0.61	-0.0007	-0.0001
	HS	0.24	0.59	0.19	0.56	0.01	0.12	0.65	0.0014	0.23	0.58	0.0077	-0.0008
	IHS	0.23	0.61	0.26	0.63	-0.0074	0.29	0.58	-0.0008	0.30	0.61	-0.0016	-0.0013
	GHS	0.21	0.63	0.25	0.63	-0.0055	0.23	0.59	0	0.26	0.61	-0.0002	-0.0008
Shiraz	SCE	0.25	0.53	0.24	0.53	0.0003	0.29	0.51	-0.0006	0.30	0.51	-0.0012	-0.0007
	HS	0.26	0.50	0.11	0.51	0.0029	0.18	0.57	0.0009	0.40	0.52	-0.0064	-0.0023
	IHS	0.27	0.51	0.3	0.51	-0.0029	0.35	0.49	-0.0017	0.18	0.52	0.0107	-0.0002
	GHS	0.20	0.58	0.24	0.55	-0.0002	0.23	0.58	-0.0004	0.37	0.46	-0.0063	-0.0007
Yazd	SCE	0.18	0.53	0.19	0.53	0.0003	0.22	0.64	-0.0006	0.24	0.65	-0.0035	-0.0007
	HS	0.20	0.64	0.31	0.62	-0.0117	0.16	0.69	0.0003	0.10	0.63	0.015	0
	IHS	0.19	0.66	0.16	0.66	0.0034	0.21	0.68	-0.0016	0.28	0.52	0.0084	-0.0015
	GHS	0.18	0.67	0.17	0.69	-0.0021	0.26	0.60	-0.0007	0.35	0.58	-0.0075	-0.0015

The statistics of the calibrated A-P coefficients in six meteorological stations (Table 3) showed that the coefficient 'a' had low values in Esfahan in the HS algorithm and high values in Bandar Abbas in the IHS algorithm. The coefficients 'a' and 'b' were predicted by four models and by four optimization algorithms. Adding T_{max}, T_{min} and RH_{mean} terms to the A-P model have had little effect on improving the radiation estimation used by the models. Zero or near-zero values of T_{max}, T_{min}, and RH_{mean} coefficients indicate this.

Table 4

Statistical comparison of calibration (Ca) and validation (Va) estimated R_s (using the locally calibrated of the models coefficients)

Station	Algorithm		A-P Model			Model1			Model2			Model3		
			RMSE	R^2	MBE	RMSE	R^2	MBE	RMSE	R^2	MBE	RMSE	R^2	MBE
Bandar Abbas	SCE	Ca	1.13	0.841	0	1.41	0.841	-0.80	1.13	0.841	0.00	1.17	0.840	0.30
		Va	1.60	0.835	-0.41	2.08	0.840	-1.25	1.60	0.835	-0.41	1.55	0.836	-0.11
	HS	Ca	1.16	0.835	0.21	1.16	0.835	-0.03	1.22	0.816	-0.01	1.25	0.823	-0.16
		Va	1.53	0.836	-0.19	1.62	0.827	-0.43	1.69	0.807	-0.42	1.63	0.818	-0.52
	IHS	Ca	1.15	0.839	-0.13	1.17	0.838	-0.23	1.18	0.833	0.15	1.20	0.821	0.08
		Va	1.69	0.832	-0.55	1.66	0.838	-0.64	1.56	0.830	-0.26	1.70	0.809	-0.34
	GHS	Ca	1.16	0.841	-0.19	1.17	0.841	-0.16	1.14	0.840	-0.09	1.35	0.825	0.62
		Va	1.61	0.839	-0.58	1.56	0.841	-0.54	1.62	0.835	-0.49	1.73	0.814	0.16
Esfahan	SCE	Ca	0.83	0.970	0.09	0.83	0.970	0.01	0.83	0.970	0.09	0.83	0.969	0.01
		Va	1.3	0.941	0.40	1.29	0.940	0.32	1.31	0.940	0.4	1.29	0.946	0.32
	HS	Ca	0.84	0.962	-0.07	0.90	0.966	-0.19	0.96	0.964	-0.02	1.13	0.943	0.12
		Va	1.26	0.940	0.24	1.29	0.937	0.14	1.40	0.935	0.26	1.53	0.923	0.36
	IHS	Ca	0.85	0.966	-0.04	0.92	0.970	0.04	0.93	0.967	0.06	0.85	0.968	0.07
		Va	1.3	0.940	0.27	1.32	0.940	0.36	1.40	0.937	0.37	1.33	0.945	0.38
	GHS	Ca	0.84	0.968	-0.12	0.83	0.970	0.01	0.87	0.970	-0.28	0.94	0.968	0.26
		Va	1.27	0.941	0.19	1.28	0.940	0.32	1.24	0.940	0.03	1.39	0.946	0.58
Kerman	SCE	Ca	1.15	0.923	-0.82	1.15	0.924	0.01	1.15	0.924	-0.13	1.14	0.925	-0.10
		Va	1.56	0.909	-0.27	1.54	0.910	-0.30	1.58	0.910	-0.43	1.55	0.911	-0.41
	HS	Ca	1.39	0.908	-1.34	1.36	0.895	-0.17	1.74	0.891	1.01	1.71	0.904	-0.34
		Va	1.23	0.895	-1.62	1.85	0.866	-0.44	1.79	0.870	0.69	1.72	0.890	-0.56
	IHS	Ca	1.22	0.908	-1.10	1.24	0.923	0.18	1.30	0.912	0.18	1.29	0.917	-0.21
		Va	1.26	0.923	-1.35	1.71	0.910	-0.17	1.74	0.897	-0.13	1.55	0.901	-0.50
	GHS	Ca	1.29	0.923	-1.32	1.15	0.924	0.10	1.16	0.923	-0.08	1.21	0.919	0.25
		Va	1.56	0.909	-1.59	1.55	0.910	-0.22	1.57	0.908	-0.38	1.50	0.907	-0.06
Mashhad	SCE	Ca	0.82	0.981	0.07	0.82	0.981	0.05	0.84	0.981	0.18	0.82	0.981	-0.10
		Va	1.24	0.961	0.07	1.24	0.960	0.08	1.26	0.961	0.17	1.25	0.961	-0.11
	HS	Ca	0.86	0.980	0.12	1.03	0.971	0.12	1.05	0.970	-0.10	1.02	0.972	-0.06
		Va	1.31	0.960	0.10	1.43	0.951	0.09	1.45	0.948	-0.10	1.34	0.952	-0.08
	IHS	Ca	0.84	0.981	0.18	0.90	0.977	-0.05	0.88	0.979	0.14	1.03	0.976	-0.12
		Va	1.26	0.960	0.17	1.30	0.957	-0.05	1.27	0.959	0.12	1.30	0.957	-0.12
	GHS	Ca	0.83	0.981	-0.04	0.86	0.979	0.03	0.87	0.981	-0.15	0.92	0.979	-0.22
		Va	1.22	0.961	-0.04	1.27	0.959	0.03	1.32	0.960	-0.17	1.25	0.959	-0.22
Shiraz	SCE	Ca	1.30	0.923	0.05	1.31	0.921	-0.18	1.28	0.923	0.05	1.27	0.923	-0.04
		Va	2.61	0.913	-2.09	2.21	0.913	-1.5	1.91	0.915	-1.03	1.95	0.916	-1.12
	HS	Ca	1.35	0.922	-0.32	2.15	0.918	-3.9	1.39	0.908	-0.03	1.48	0.911	0
		Va	2.99	0.912	-2.50	5.38	0.909	-5.09	2.15	0.899	-1.27	1.82	0.904	-0.86
	IHS	Ca	1.32	0.922	0.20	1.40	0.917	0.45	1.35	0.917	0.02	1.38	0.913	-0.11
		Va	2.54	0.912	-1.97	1.90	0.912	-0.75	1.83	0.909	-0.91	2.04	0.900	-1.16
	GHS	Ca	1.38	0.923	-0.33	1.30	0.921	0.15	1.37	0.922	0.06	1.4	0.917	-0.21
		Va	2.85	0.913	-2.41	1.90	0.913	-0.98	1.79	0.915	-0.96	2.28	0.913	-1.39
Yazd	SCE	Ca	2.67	0.921	-2.36	2.21	0.921	-2.65	1.51	0.924	0.04	1.50	0.925	0.02
		Va	2.39	0.916	-2.68	2.11	0.916	-2.33	1.72	0.919	0.48	1.71	0.920	0.51
	HS	Ca	2.03	0.920	-1.39	1.73	0.913	-0.30	1.58	0.919	0.15	1.69	0.904	-0.04
		Va	1.75	0.913	0.36	1.99	0.910	0.81	1.78	0.918	0.55	1.86	0.897	0.20
	IHS	Ca	1.94	0.921	-1.25	1.55	0.920	-0.05	1.70	0.920	-0.24	1.73	0.905	0.16
		Va	1.76	0.914	0.52	1.72	0.914	0.32	1.75	0.915	0.30	1.99	0.899	0.50
	GHS	Ca	2.00	0.921	-1.32	1.56	0.922	-0.26	1.56	0.924	0.25	1.59	0.920	0.19
		Va	1.73	0.915	0.45	1.66	0.917	0.19	1.84	0.919	0.67	1.88	0.915	0.73

RMSE (MJ $m^{-2}day^{-1}$), MBE (MJ $m^{-2}day^{-1}$)

3.1.Evaluation of solar radiation (R_s) estimation models

In the studied stations, the values of R^2, RMSE, and MBE for the calibrated models showed in Table 4. When tested using the R^2 value, the calibrated models were found to execute best in Mashhad, followed by Esfahan, Shiraz, Yazd, Kerman, and Bandar Abbas. Due to the inaccuracy in recording and a large number of discarded data in Bandar Abbas station, this station did not have very good results compared to other stations. The RMSE performance indicated that the calibrated models had the smallest error in Mashhad, followed by Esfahan, Bandar Abbas, Kerman, Shiraz, and Yazd. The mean RMSE values for the three improved models were lower than 1.3, which also indicated acceptable exactitude. The mean R^2 value of the improved models was largest in Mashhad (0.977), followed by the values for Esfahan, Shiraz, Yazd, Kerman, and Bandar Abbas. The performance of the improved models in the same climates showed very small variation. The RMSE statistic showed that all models were more accurate in Esfahan, with an average value of 0.89 MJ m^{-2} day^{-1}, followed by Bandar Abbas, Mashhad, Shiraz, Kerman, and Yazd. The fact that all improve models validated by the two statistical indicators performed well and that there was no significant difference between the models in each station show that these two indicators could not be used alone to specify the best model in each station. Therefore, the MBE statistic was used to determine the difference between the estimated and measured data. Based on Performance indicators RMSE, MBE, calibration of the A-P model improved the accuracy of estimated R_s in most of the studied stations. If the value of R^2 and RMSE are closer to one and zero respectively, the model is more appropriate.

3.2.Comparison of results with other researchers

Calibrated the coefficients of the A-P model by various researchers showed in Table 5. In this research, the coefficients 'a' and 'b' were calculated for the selected stations with different

optimization algorithms (Table 3). Coefficient 'a' varies from 0.13 to 0.39, Also coefficient 'b' varies from 0.33 to 0.67 for six stations.

Table 5

Comparison of calibrated coefficients of the A-P model in the present study with the results of other researchers

Station		Bandar Abbas		Esfahan		Shiraz		Kerman		Mashhad		Yazd	
		a	b	a	b	a	b	a	b	a	b	a	b
Khalili and Rezai-e Sadr (1997)				0.30	0.42	0.29	0.42	0.28	0.45	0.30	0.37	0.21	0.64
Javadi and Moeini (2010)		0.34	0.306	0.361	0.35	0.317	0.405	0.322	0.421	0.335	0.332	0.345	0.398
Sabziparvar et al (2013)				0.271	0.48	0.247	0.512	0.267	0.518	0.274	0.418	0.304	0.492
Didari and Ahmadi (2019)						0.31	0.48						
Present study	SCE	0.38	0.35	0.15	0.58	0.25	0.53	0.27	0.51	0.22	0.62	0.18	0.53
	HS	0.38	0.36	0.13	0.60	0.26	0.50	0.28	0.47	0.24	0.59	0.20	0.64
	IHS	0.39	0.33	0.16	0.56	0.27	0.51	0.24	0.54	0.23	0.61	0.19	0.66
	GHS	0.36	0.37	0.15	0.57	0.20	0.58	0.26	0.50	0.21	0.63	0.18	0.67

In comparison with previous researches, some differences were observed between the results of this research and other works. For example, Javadi and Moeini (2010), Sabziparvar et al. (2013), and Khalili and Rezai-e Sadr (1997) applied the A-P model for Shiraz and reported the following pairs of 'a' and 'b', 0.317, 0.405; 0.247, 0.512; 0.29, 0.42, respectively. Whiles in the present research values of 'a' and 'b' coefficients were obtained as 0.25 and 0.53 with the SCE optimization algorithm for the same station; that is in good agreement with the coefficients of Sabziparvar et al. In this research, the A-P coefficients 'a' and 'b' with the SCE optimization algorithm were obtained 0.22 and 0.62 for Mashhad, but Khalili and Rezai-e Sadr (1997), Javadi and Moeini (2010) and Sabziparvar et al. (2013) reported, 0.30, 0.37; 0.335,.0.332 and 0.274,0.418 for the same station, respectively. Javadi and Moeini (2010), Sabziparvar et al. (2013), and Khalili and Rezai-e Sadr (1997) suggested the application of the A-P model for the Esfahan station with the following pairs of coefficients 'a' and 'b': 0.361, 0.35; 0.271, 0.482; and 0.30, 0.42; but this research suggests values of 0.15 and 0.58 for 'a' and 'b' with the SCE optimization algorithm, respectively (Table 3). The inconsistency of the results can be explained by a longer period of estimated R_s, which were applied in this research. Based on Liu et al. (2009), sample size and the length of the observation period could illustrate such

differences in different researches. Also, the rules for quality control of the R_s dataset and the higher restrictions for removing unreliable R_s data might somewhat cause such discrepancies (Table 5).

The values of measured and estimated global solar radiation by the A-P model from 1992 to 2017 are compared as shown in Fig. 4. To appraise the prediction accuracy of R_s, computed from the regional best performing estimated data and the measured data, specific values of the A-P model statistics by different optimization algorithms (HS, IHS, GHS, and SCE) in the Kerman station were compared. Also, the R^2 values of both the measured data and the estimated data in this station were very close to the 1:1 line, which means that the R_s determined from the estimated data and measured data were in good accordance.

According to Table 4 and Fig. 4, the calibration and validation performance of the A-P model was better than three improved models in all stations. As shown in Table 4, the RMSE varies between 0.82 and 2.67 MJ $m^{-2}day^{-1}$ for the A-P model with the SCE algorithm in the calibration phase. Besides, other indicators were lower in the case of the A-P models in the SCE algorithm. Based on the results in Tables 4 and Table 5, the decrease rate of RMSE values in various stations for four optimization algorithms was different. For example, in the SCE algorithm, the value of RMSE decreased by about 4% and 7% for Mashhad and Kerman stations in the calibration phase contrasted to the HS algorithm, respectively. In other words, the highest decrease of RMSE is related to Kerman station. The lowest value of R^2 was observed in Bandar Abbas station (R^2 = 0.81). Further, according to MBE values, a decrease occurred in the MBE of all stations in the SCE algorithm contrasted to three algorithms (IHS, GHS, and Hs), in the A-P and three improved models.

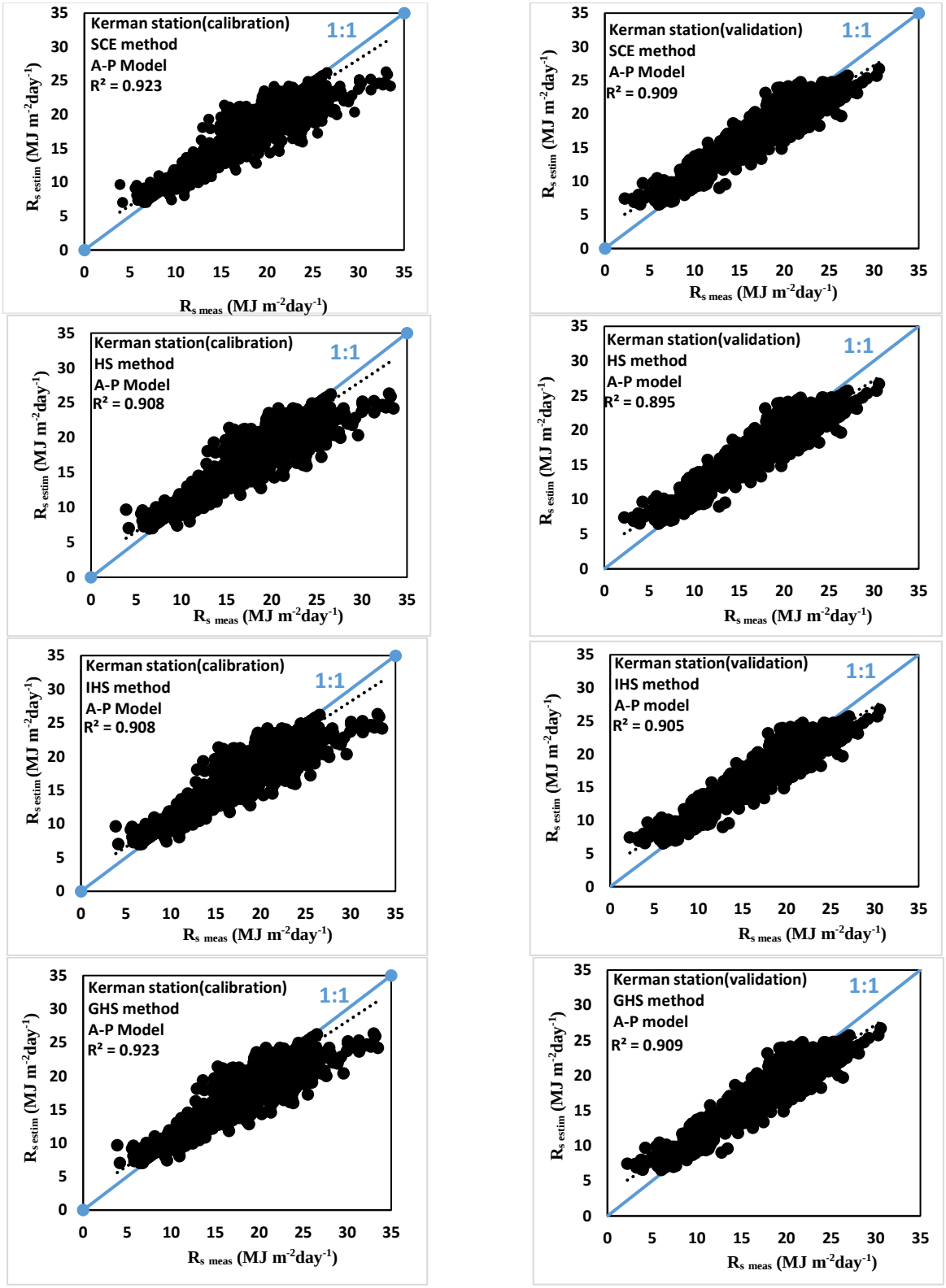

Fig. 4. Comparison of measured and estimated R_s in the A-P model

According to Table 4 and Fig. 4, the calibration and validation performance of the A-P model was better than three improved models in all stations. As shown in Table 4, the RMSE varies between 0.82 and 2.67 MJ $m^{-2}day^{-1}$ for the A-P model with the SCE algorithm in the calibration

phase. Besides, other indicators were lower in the case of the A-P models in the SCE algorithm. Based on the results in Tables 4 and Table 5, the decrease rate of RMSE values in various stations for four optimization algorithms was different. For example, in the SCE algorithm, the value of RMSE decreased by about 4% and 7% for Mashhad and Kerman stations in the calibration phase contrasted to the HS algorithm, respectively. In other words, the highest decrease of RMSE is related to Kerman station. The lowest value of R^2 was observed in Bandar Abbas station (R^2 = 0.81). Further, according to MBE values, a decrease occurred in the MBE of all stations in the SCE algorithm contrasted to three algorithms (IHS, GHS, and Hs), in the A-P and three improved models.

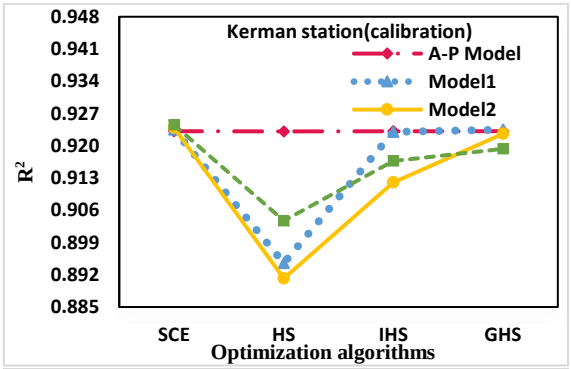

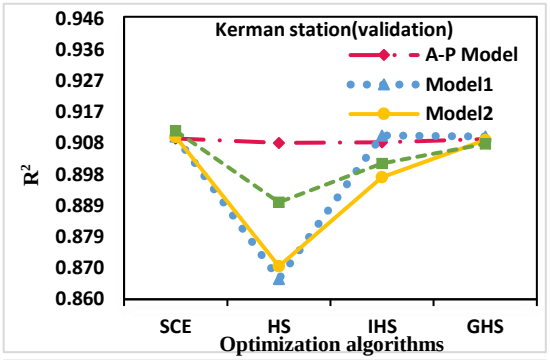

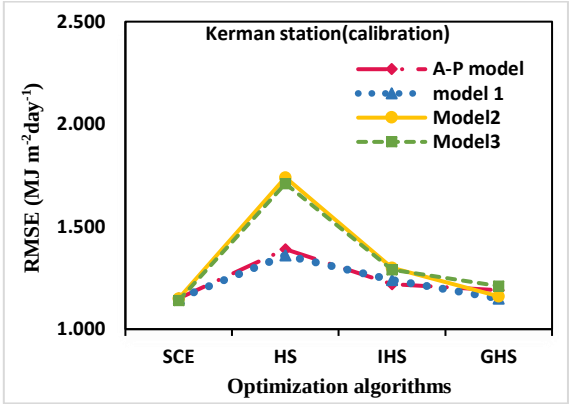

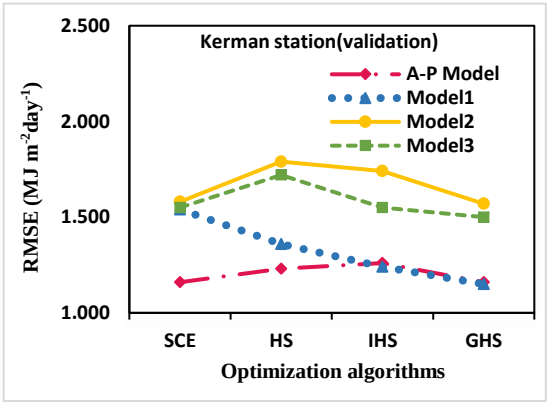

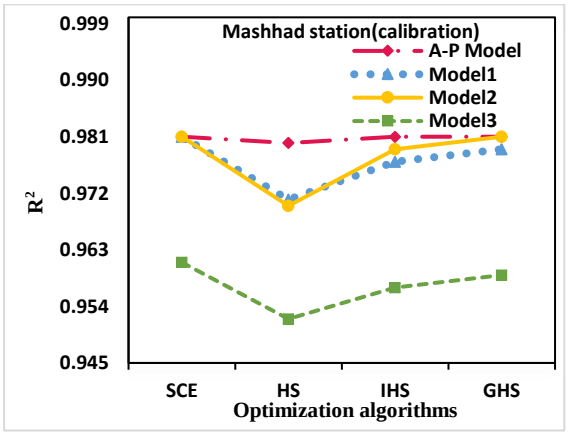

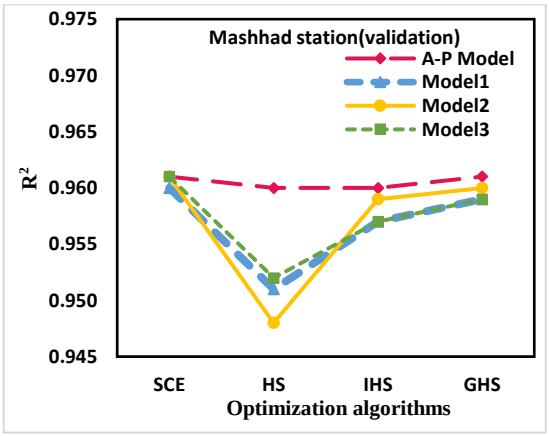

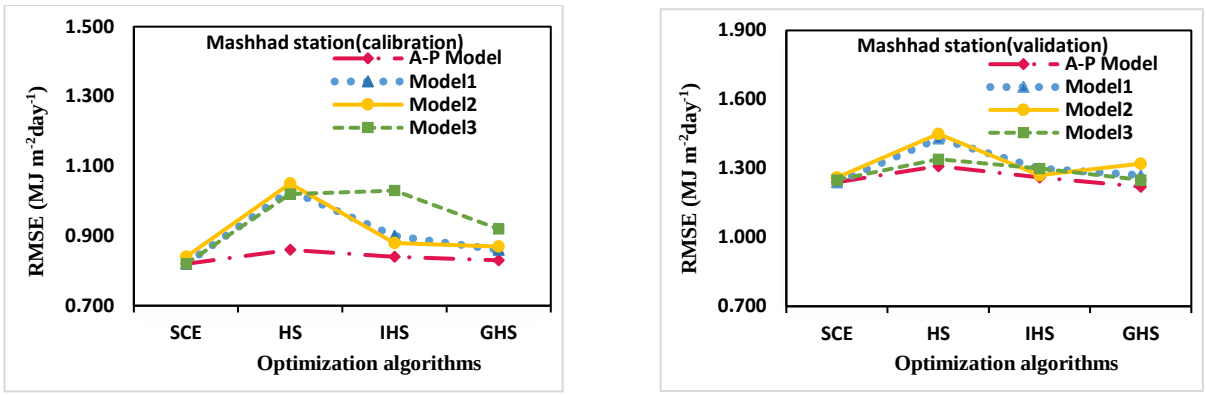

Fig. 5. Comparison R^2 and RMSE between the calibrated and validation model with different optimization algorithms for Mashhad and Kerman stations

The values of R^2 and RMSE for Mashhad and Kerman stations by different optimization algorithms, the A-P model, and the three improved models are shown in Fig. 5.

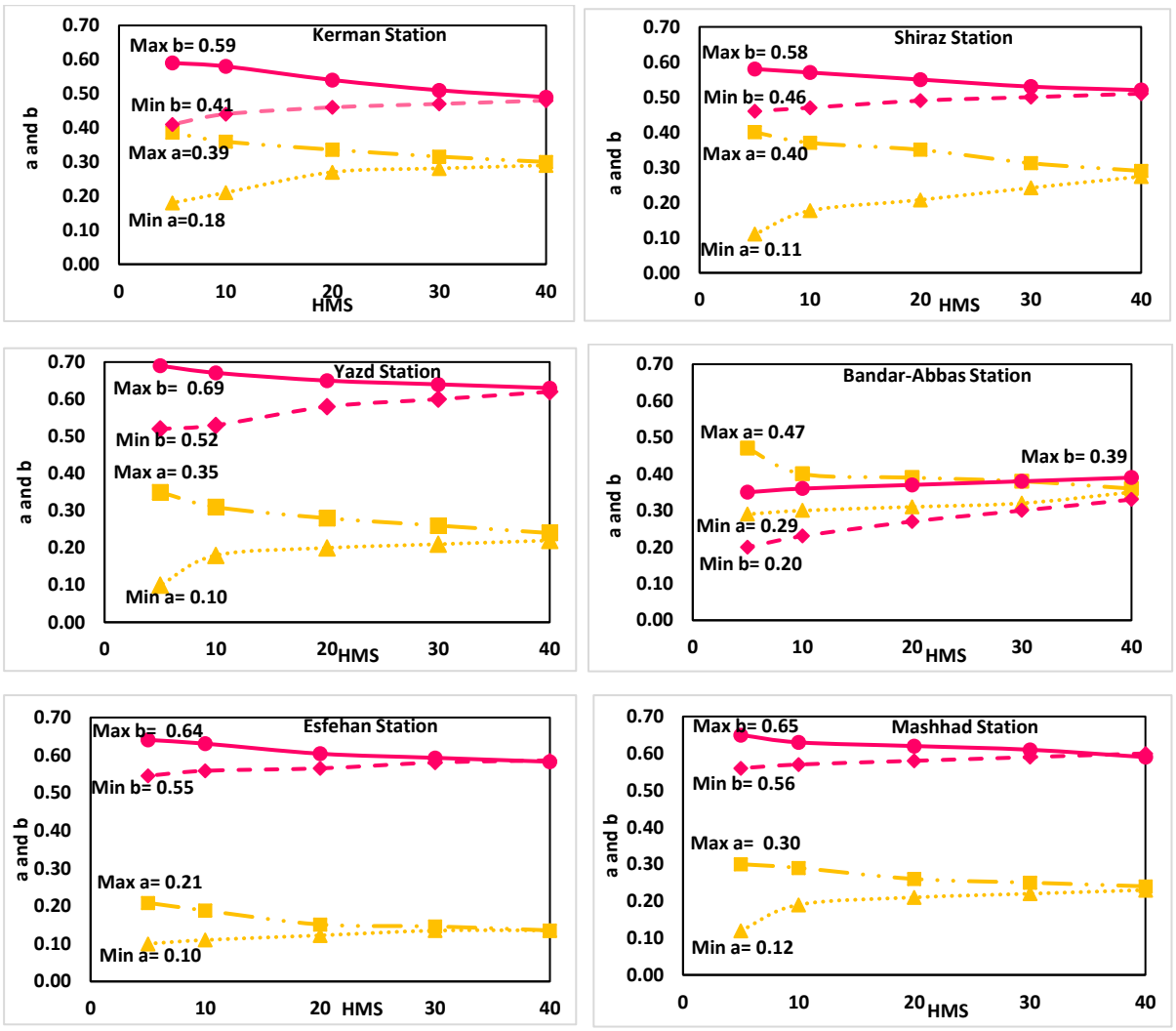

Fig6. The minimum and maximum A-P model coefficients in Hs method, in different harmony memory size (HMS)

The values of 'a' and 'b' in the harmonic memory sizes (HMS) (5, 10, 20, 30, and 40) in six meteorological stations are shown in Fig. 6. This Figure show that as the initial population increases, the values of the coefficients become convergent and a smaller range for the coefficients is obtained in different stations. For example, in Kerman station, with increasing HMS, the minimum and maximum coefficient 'a', changes from 0.18 to 0.35 and from 0.39 to 0.36, respectively. The maximum and minimum values of 'a' are close to each other, and this is true for coefficient 'b'.

4. **Conclusion**

The results of the based on daily R_s and meteorological data from six stations in Iran from 1992–2017, the performance of the calibrated A-P model, and three improved models for the A-P coefficients were evaluated, and the best performing those for each station were obtained. For practical usages, the use of a calibrated form of the A-P model seems necessary for Iran climatic situations.

The effect of T and RH was applied to the A-P model and the coefficients of these models were calibrated by optimization methods. The results showed that adding T_{max}, $T_{min,}$ and RH_{mean} did not have much effect on the A-P model. Also, the SCE optimization algorithm method has shown better results than other optimization methods.

Considering the sunshine, which is an important factor for estimating R_s, and accepting that Iran is a country in which sunshine is significant, the Angstrom empirical model can well estimate total radiation. In this research, the coefficients 'a' and 'b' were calibrated. Coefficient 'a' varies from 0.1 to 0.47 and coefficient 'b' varies from 0.2 to 0.69 for studied stations.

In this research, three R_s estimation models were appraised and calibrated. The results indicate that, among the improved models, the A-P model (R^2 = 0.981 in Mashhad station) offers the best R_s estimations in the semi-arid and arid climate, as compared to the measured R_s.

5. Reference

Abraha, M. G., & Savage, M. J. (2008). Comparison of estimates of daily solar radiation from air temperature range for application in crop simulations. *Agricultural and Forest Meteorology*, *148*(3), 401–416. https://doi.org/10.1016/j.agrformet.2007.10.001

Abualigah, L., Diabat, A., & Geem, Z. W. (2020). A comprehensive survey of the harmony search algorithm in clustering applications. *Applied Sciences (Switzerland)*, *10*(11), 1–26. https://doi.org/10.3390/app10113827

Adeyeri, O. E., Laux, P., Arnault, J., Lawin, A. E., & Kunstmann, H. (2020). Conceptual hydrological model calibration using multi-objective optimization techniques over the transboundary Komadugu-Yobe basin, Lake Chad Area, West Africa. *Journal of Hydrology: Regional Studies*, *27*(December 2019), 100655. https://doi.org/10.1016/j.ejrh.2019.100655

Ağbulut, Ü., Gürel, A. E., & Biçen, Y. (2021). Prediction of daily global solar radiation using different machine learning algorithms: Evaluation and comparison. *Renewable and Sustainable Energy Reviews*, 135(July 2020). https://doi.org/10.1016/j.rser.2020.110114

Aghashariatmadari, Z., Khalili, A., Irannejad, P., Liaghat, A. (2012). Calibration and Annual Changes of the Coefficients of the Angstrom-Prescott (A-P) Equation ('a' and 'b') in Different Time Scales. *Journal of Water and soil* 25, 905–911.

Alshammari, N., & Asumadu, J. (2020). Optimum unit sizing of hybrid renewable energy system utilizing harmony search, Jaya, and particle swarm optimization algorithms. *Sustainable Cities and Society*, *60*(November 2019), 102255. https://doi.org/10.1016/j.scs.2020.102255

Ayvaz, M. T. (2010). A linked simulation-optimization model for solving the unknown groundwater pollution source identification problems. *Journal of Contaminant Hydrology*, *117*(1–4), 46–59. https://doi.org/10.1016/j.jconhyd.2010.06.004

406 Allen, R.G., Pereira, L.S., Raes, D., Smith, M. (1998). Crop Evapotranspiration-Guidelines
407 for Computing Crop Water Requirements-FAO Irrigation and Drainage Paper 56; *Food*
408 *and Agriculture Organization of the United Nations: Rome, Italy* 300, D05109.
409 http://www.fao.org/docrep
410 Angstrom A. (1924). Solar and atmospheric radiation. *Quarterly Journal of the Royal*
411 *Meteorological Society* 50, 121-126.
412 Bashiri-Atrabi, H., Qaderi, K., Rheinheimer, D. E., & Sharifi, E. (2015). Application of
413 Harmony Search Algorithm to Reservoir Operation Optimization. *Water Resources*
414 *Management*, *29*(15), 5729–5748. https://doi.org/10.1007/s11269-015-1143-3
415 Besharat, F., Dehghan, A. A., & Faghih, A. R. (2013). Empirical models for estimating
416 global solar radiation: A review and case study. *Renewable and Sustainable Energy*
417 *Reviews*, *21*, 798–821. https://doi.org/10.1016/j.rser.2012.12.043
418 Boscaini, R., Robaina, A. D., Peiter, M. X., Bruning, J., Rodrigues, S. A., da Silva, J. G.,
419 Medeiros, E. P., & Piroli, J. D. (2020). Performance of solar radiation models for
420 obtaining reference evapotranspiration to Santa Maria-RS, Brazil. *Revista Brasileirade*
421 *Ciencias Agrarias*, *15*(1), 1–8. https://doi.org/10.5039/AGRARIA.V15I1A7661
422 Chang, K., & Zhang, Q. (2020). Development of a solar radiation model considering the
423 hourly sunshine duration for all-sky conditions – A case study for Beijing, China.
424 *Atmospheric Environment*, *234*(May), 117617.
425 https://doi.org/10.1016/j.atmosenv.2020.117617
426 Chen, J. L., He, L., Wen, Z. F., Lv, M. Q., Yi, X. X., & Wu, S. J. (2018). A general empirical
427 model for estimation of solar radiation in the Yangtze river basin. *Applied Ecology and*
428 *Environmental Research*, *16*(2), 1471–1482.
429 https://doi.org/10.15666/aeer/1602_14711482
430 Chen, Ji Long, & Li, G. S. (2013). Estimation of monthly average daily solar radiation from

measured meteorological data in the Yangtze River Basin in China. *International Journal of Climatology*, *33*(2), 487–498. https://doi.org/10.1002/joc.3442

Chen, R., Ersi, K., Yang, J., Lu, S., & Zhao, W. (2004). Validation of five global radiation models with measured daily data in China. *Energy Conversion and Management*, *45*(11–12), 1759–1769. https://doi.org/10.1016/j.enconman.2003.09.019

Čistý, M. (2008). Automated calibration of the simulation model of irrigation projects by harmony search optimization. *Journal of Water and Land Development*, *12*(12), 3–13. https://doi.org/10.2478/v10025-009-0001-1

Cui, L. J., & Kuczera, G. (2003). Optimizing urban water supply headworks using probabilistic search methods. *Journal of Water Resources Planning and Management*, *129*(5), 380–387. https://doi.org/10.1061/(ASCE)0733-9496(2003)129:5(380)

Cunha, A. C., Filho, L. R. A. G., Tanaka, A. A., Goes, B. C., & Putti, F. F. (2021). Influence of the Estimated Global Solar Radiation on the Reference Evapotranspiration Obtained Through the Penman-Monteith Fao 56 Method. *Agricultural Water Management*, 243(August 2020). https://doi.org/10.1016/j.agwat.2020.106491

De Souza, J. L., Lyra, G. B., Dos Santos, C. M., Ferreira Junior, R. A., Tiba, C., Lyra, G. B., & Lemes, M. A. M. (2016). Empirical models of daily and monthly global solar irradiation using sunshine duration for Alagoas State, Northeastern Brazil. *Sustainable Energy Technologies and Assessments*, *14*, 35–45. https://doi.org/10.1016/j.seta.2016.01.002

Didari, S., & Ahmadi, S. H. (2019). Calibration and evaluation of the FAO56 Penman-Monteith, FAO24-radiation, and Priestly-Taylor reference evapotranspiration models using the spatially measured solar radiation across a largely arid and semi-arid area in southern Iran. *Theoretical and Applied Climatology*, *136*(1–2), 441–455. https://doi.org/10.1007/s00704-018-2497-2

Duan, Q., Sorooshian, S., & Gupta, V. (1992). Effective and Efficient Global Optimization. *Water Resources Research*, *28*(4), 1015–1031.

Duan, Q.Y., Gupta, V.K., Sorooshian, S. (1993). Shuffled complex evolution approach for effective and efficient global minimization. *Journal of Optimization Theory and Applications*, 76(3), 501-521. https://doi.org/10.1007/bf00939380

Elshaboury, N., Attia, T., & Marzouk, M. (2020). *Application of Evolutionary Optimization Algorithms for Rehabilitation of Water Distribution Networks*. *146*(7), 1–11. https://doi.org/10.1061/(ASCE)CO.1943-7862.0001856

Fan, J., Wu, L., Zhang, F., Cai, H., Ma, X., & Bai, H. (2019). Evaluation and development of empirical models for estimating daily and monthly mean daily diffuse horizontal solar radiation for different climatic regions of China. *Renewable and Sustainable Energy Reviews*, 105(December 2018), 168–186. https://doi.org/10.1016/j.rser.2019.01.040

Geem, Z. W. (2007). Optimal scheduling of multiple dam systems using a harmony search algorithm. *Lecture Notes in Computer Science (Including Subseries Lecture Notes in Artificial Intelligence and Lecture Notes in Bioinformatics)*, *4507 LNCS*, 316–323.

Geem, Z.W., Kim, J.H., Loganathan, G.V. (2001). A New Heuristic Optimization Algorithm: Harmony Search. SIMULATION, 76, 60-68.

He, C., Liu, J., Xu, F., Zhang, T., Chen, S., Sun, Z., Zheng, W., Wang, R., He, L., Feng, H., Yu, Q., & He, J. (2020). Improving solar radiation estimation in China based on regional optimal combination of meteorological factors with machine learning methods. *Energy Conversion and Management*, *220*(June), 113111. https://doi.org/10.1016/j.enconman.2020.113111

Holland, J. H. (1975). Adaptation in Natural and Artificial Systems, University of Michigan Press, Ann Arbor, Michigan.

Jahani, B., Dinpashoh, Y., & Wild, M. (2018). Dimming in Iran since the 2000s and the

potential underlying causes. *International Journal of Climatology*, *38*(3), 1543–1559. https://doi.org/10.1002/joc.5265

Jahani, B., & Mohammadi, B. (2018). A comparison between the application of empirical and ANN methods for estimation of daily global solar radiation in Iran. *Theoretical and Applied Climatology* 137, 1257-1269. https://doi.org/10.1007/s00704-018-2666-3

Jamil, B., Irshad, K., Algahtani, A., Islam, S., Ali, M. A., & Shahab, A. (2019). On the calibration and applicability of global solar radiation models based on temperature extremities in India. *March*, 1–13. https://doi.org/10.1002/ep.13236

Javadi, S., Moeini, S. (2010). A new solar radiation models for Iran. Conference paper, 106-110.

Khalili, A., Rezaei-Sadr, H. (1997). Estimation of global solar radiation over Iran based on climatological data. 46, 15-35.

Kisi, O., Alizamir, M., (2018). Modelling reference evapotranspiration using a new wavelet conjunction heuristic method: Wavelet extreme learning machine vs wavelet neural networks. *Agricultural and Forest Meteorology*. 263, 41–48. https://doi.org/10.1016/j.agrformet.2018.08.007

Liu, D. L., & Scott, B. J. (2001). Estimation of solar radiation in Australia from rainfall and temperature observations. *Agricultural and Forest Meteorology*, *106*(1), 41–59. https://doi.org/10.1016/S0168-1923(00)00173-8

Liu, J., Pan, T., Chen, D., Zhou, X., Yu, Q., Flerchinger, G. N., Liu, D. L., Zou, X., Linderholm, H. W., Du, J., Wu, D., & Shen, Y. (2017). An Improved ångström-type model for estimating solar radiation over the tibetan plateau. *Energies*, *10*(7). https://doi.org/10.3390/en10070892

Liu, X., Mei, X., Li, Y., Wang, Q., Zhang, Y., & Porter, J. R. (2009). Variation in reference crop evapotranspiration caused by the Ångström-Prescott coefficient: Locally calibrated

versus the FAO recommended. *Agricultural Water Management*, *96*(7), 1137–1145. https://doi.org/10.1016/j.agwat.2009.03.005

Liu, Y., Tan, Q., & Pan, T. (2019). Determining the Parameters of the Ångström-Prescott Model for Estimating Solar Radiation in Different Regions of China: Calibration and Modeling. *Earth and Space Science*, *6*(10), 1976–1986. https://doi.org/10.1029/2019EA000635

Luo, Q., Yang, Y., Qian, J., Wang, X., Chang, X., Ma, L., Li, F., & Wu, J. (2020). Spring protection and sustainable management of groundwater resources in a spring field. *Journal of Hydrology*, *582*(December 2019), 124498. https://doi.org/10.1016/j.jhydrol.2019.124498

Mahdavi, M., Fesanghary, M., & Damangir, E. (2007). An improved harmony search algorithm for solving optimization problems. *Applied Mathematics and Computation*, *188*(2), 1567–1579. https://doi.org/10.1016/j.amc.2006.11.033

Mihalakakou, G., Santamouris, M., & Asimakopoulos, D. N. (2000). The total solar radiation time series simulation in Athens, using neural networks. *Theoretical and Applied Climatology*, *66*(3–4), 185–197. https://doi.org/10.1007/s007040070024

Moradi, I. (2009). Quality control of global solar radiation using sunshine duration hours. *Energy*, *34*(1), 1–6. https://doi.org/10.1016/j.energy.2008.09.006

Mousavi, R., Sabziparvar, A. A., Marofi, S., Ebrahimi Pak, N. A., & Heydari, M. (2014). Calibration of the Angström-Prescott solar radiation model for accurate estimation of reference evapotranspiration in the absence of observed solar radiation. *Theoretical and Applied Climatology*, *119*(1–2), 43–54. https://doi.org/10.1007/s00704-013-1086-7

Ododo, J. C., Sulaiman, A. T., Aidan, J., Yuguda, M. M., & Ogbu, F. A. (1995). The importance of maximum air temperature in the parameterization of solar radiation in Nigeria. *Renewable Energy*, *6*(7), 751–763. https://doi.org/10.1016/0960-

1481(94)00097-P

Ojosu, J.O., Komolafe, L.K. (1987). Models for estimating solar radiation availability in South-Western Nigeria. *Nigeria Journal Solar Energy*, 6, 69–77.

Omran, M., Mahdavi, M. (2008). Global-best harmony search. A*pplied Mathematics and Computation*, 198, 643-656.

Paulescu, M., Stefu, N., Calinoiu, D., Paulescu, E., Pop, N., Boata, R., & Mares, O. (2016). Ångström-Prescott equation: Physical basis, empirical models, and sensitivity analysis. *Renewable and Sustainable Energy Reviews*, *62*, 495–506. https://doi.org/10.1016/j.rser.2016.04.012

Pellicone, G., Caloiero, T., & Guagliardi, I. (2019). The De Martonne aridity index in Calabria (Southern Italy). *Journal of Maps*, *15*(2), 788–796. https://doi.org/10.1080/17445647.2019.1673840

Prescott, J.A (1940). Evaporation from a Water Surface in Relation to Solar Radiation. Transactions of the Royal Society of South Australia, 64, 114-118.

Rahimi, I., Bakhtiari, B., Qaderi, K., & Aghababaie, M. (2012). Calibration of angstrom equation for estimating solar radiation using the Meta-Heuristic Harmony Search Algorithm (Case study: Mashhad-east of Iran). *Energy Procedia*, *18*(1), 644–651. https://doi.org/10.1016/j.egypro.2012.05.078

Rahimi, J., Ebrahimpour, M., & Khalili, A. (2013). Spatial changes of Extended De Martonne climatic zones affected by climate change in Iran. *Theoretical and Applied Climatology*, *112*(3–4), 409–418. https://doi.org/10.1007/s00704-012-0741-8

Raoof, M., & Mobaser, J. A. (2019). Reference evapotranspiration estimation using a locally adjusted coefficient of angstrom's radiation model in an arid-cold region. *Journal of Agricultural Science and Technology*, *21*(2), 487–499.

Robaa, S. M. (2009). Validation of the existing models for estimating global solar radiation

over Egypt. *Energy Conversion and Management*, *50*(1), 184–193. https://doi.org/10.1016/j.enconman.2008.07.005

Sabziparvar, Ali A., & Shetaee, H. (2007). Estimation of global solar radiation in arid and semi-arid climates of East and West Iran. *Energy*, *32*(5), 649–655. https://doi.org/10.1016/j.energy.2006.05.005

Sabziparvar, Ali Akbar, Mousavi, R., Marofi, S., Ebrahimipak, N. A., & Heidari, M. (2013). An Improved Estimation of the Angstrom-Prescott Radiation Coefficients for the FAO56 Penman-Monteith Evapotranspiration Method. *Water Resources Management*, *27*(8), 2839–2854. https://doi.org/10.1007/s11269-013-0318-z

Sanchez-Lorenzo, A., Enriquez-Alonso, A., Wild, M., Trentmann, J., Vicente-Serrano, S. M., Sanchez-Romero, A., Posselt, R., & Hakuba, M. Z. (2017). Trends in downward surface solar radiation from satellites and ground observations over Europe during 1983–2010. *Remote Sensing of Environment*, *189*, 108–117. https://doi.org/10.1016/j.rse.2016.11.018

Sanikhani, H., Kisi, O., Maroufpoor, E., & Yaseen, Z. M. (2019). Temperature-based modeling of reference evapotranspiration using several artificial intelligence models: application of different modeling scenarios. *Theoretical and Applied Climatology*, *135*(1–2), 449–462. https://doi.org/10.1007/s00704-018-2390-z

Shamshirband, S., Mohammadi, K., Chen, H. L., Narayana Samy, G., Petković, D., & Ma, C. (2015). Daily global solar radiation prediction from air temperatures using kernel extreme learning machine: A case study for Iran. *Journal of Atmospheric and Solar-Terrestrial Physics*, 134, 109–117. https://doi.org/10.1016/j.jastp.2015.09.014

Şen, Z., Öztopal, A., & Şahin, A. D. (2001). Application of genetic algorithm for the determination of Angstrom equation coefficients. *Energy Conversion and Management*, *42*(2), 217–231. https://doi.org/10.1016/S0196-8904(00)00041-8

Şenkal, O., & Kuleli, T. (2009). Estimation of solar radiation over Turkey using artificial neural network and satellite data. *Applied Energy*, *86*(7–8), 1222–1228. https://doi.org/10.1016/j.apenergy.2008.06.003

Tabari, H., Hosseinzadehtalaei, P., Willems, P., & Martinez, C. (2016). Validation and calibration of solar radiation equations for estimating daily reference evapotranspiration at cool semi-arid and arid locations. *Hydrological Sciences Journal*, *61*(3), 610–619. https://doi.org/10.1080/02626667.2014.947293

Weiss, A., & Hays, C. J. (2004). Simulation of daily solar irradiance. *Agricultural and Forest Meteorology*, *123*(3–4), 187–199. https://doi.org/10.1016/j.agrformet.2003.12.002

Yin, Y., Wu, S., Zheng, D., & Yang, Q. (2008). Radiation calibration of FAO56 Penman-Monteith model to estimate reference crop evapotranspiration in China. *Agricultural Water Management*, *95*(1), 77–84. https://doi.org/10.1016/j.agwat.2007.09.002

Zhang, Y., Li, X., & Bai, Y. (2015). An integrated approach to estimate shortwave solar radiation on clear-sky days in rugged terrain using MODIS atmospheric products. *Solar Energy*, *113*, 347–357. https://doi.org/10.1016/j.solener.2014.12.028

608 The performance of the A-P model had more precision and less error than improved models in all the stations in
609 this research

610 The best performance of the A-P model was obtained with the Shuffled Complex Evolution (SCE) algorithm.

611 Sunshine was the main factor determining the solar radiation